Sensitivity analysis of transient diesel engine simulation

C D Rakopoulos* and **E G Giakoumis**
Department of Thermal Engineering, School of Mechanical Engineering, National Technical University of Athens, Athens, Greece

The manuscript was received on 25 April 2005 and was accepted after revision for publication on 25 August 2005.

DOI: 10.1243/095440705X69641

Abstract: An experimentally validated simulation code is used to study the errors induced by various, usually applied, modelling simplifications in the prediction of diesel engine operation under transient conditions after a ramp increase in load. The following simulation cases are investigated: multicylinder engine modelling, with the equations of each cylinder solved separately during each transient cycle; cylinder wall temperature modelling, with the analytical heat convection–conduction scheme compared with the usual constant wall temperature approach; in-cylinder radiation temperature correction to compensate for the underestimation of maximum temperatures from single-zone modelling; mathematical fuel pump modelling in contrast to steady state fuel injection curves; friction modelling during a transient event simulated using equations per degree crank angle as opposed to the 'mean' f.m.e.p. approach; and 'deterioration' scenarios applied to both friction and combustion rates to compensate for the peculiarities of transient operation. It is revealed that the multicylinder, analytical friction, and detailed fuel pump modelling can have an important effect on the prediction of diesel engine transient operation and thus should not be excluded from a complete transient model. The cylinder wall temperature simulation used only marginally affects the prediction of transients, whereas the friction and combustion deterioration can have quite dramatic results but need further experimental validation.

Keywords: sensitivity analysis, turbocharged diesel engine, transient operation, multicylinder, heat conduction, radiation temperature, friction, fuel pump

1 INTRODUCTION – OBJECTIVES

The turbocharged compression ignition (diesel) engine is the most preferred prime mover in medium and medium-large unit applications owing to its reliability which is combined with excellent fuel efficiency. Nonetheless, its transient operation is often linked with off-design (e.g. turbocharger lag) and consequently non-optimum performance, pointing out the significance of proper interconnection between engine, governor, fuel pump, turbocharger, and load.

During the last decades, diesel engine modelling and experimental investigation have paved the way for an in-depth study of transient operation [**1–11**]. These works have dealt, in particular, with the study of the effect of various parameters [**3**, **4**, **6**, **11**], the effect of governor design [**7**], two-stroke engine operation [**1**], experimental [**5**, **8**] and predicted [**9**] emissions, and second-law analysis [**10**].

Transient simulation codes suffer from the need to run a large number of engine cycles, particularly when transient cycles analysis is involved, a fact usually limiting the main simulation philosophy to single-zone or two-zone modelling. This often results in ignoring or simplifying specific submodels for the sake of speeding up program execution. These simplifications can be justified if the goal is to identify key parameters that influence transient response or just general trends. However, these can prove quite limiting if the scope is an in-depth study of transient phenomena, especially today when stringent regulations concerning engine exhaust emissions dominate the associated industry.

* *Corresponding author: Internal Combustion Engines Laboratory, Department of Thermal Engineering, School of Mechanical Engineering, National Technical University of Athens, 9 Heron Polytechniou Str., Zografou Campus, 15780 Athens, Greece. email: cdrakops@central.ntua.gr*

Typical modelling simplifications include:

(a) single-zone modelling;
(b) the assumption of constant cylinder wall temperature throughout the whole transient test;
(c) the solution of the equations of one cylinder by assuming that all the others behave in the same way for each transient cycle;
(d) the use of steady state fuel injection data;
(e) the use of steady state turbocharger data;
(f) the use of steady state dynamometer curves;
(g) filling and emptying modelling of exhaust manifold operation;
(h) the simulation of friction torque with the use of mean friction mean effective pressure (f.m.e.p.) relations;
(i) assumptions that both combustion and friction behave during transients in the same way as they do under steady state operation.

It is the intention of the present work to investigate many of the above simplifications in order to be able to estimate their validity and evaluate their importance in transient simulation codes. To this end, firstly a multicylinder engine modelling scheme is applied where all differential and algebraic equations are solved separately and sequentially for each cylinder. By so doing, the 'single-cylinder' solution approach will be put to the test and possible differences in the performance of cylinders during the same engine cycle of a transient event will be revealed.

The cylinder wall temperature profile adopted, i.e. a constant wall temperature assumption as opposed to a detailed heat convection–conduction scheme, will be studied, as well as the use of corrected radiation temperatures during combustion to compensate for the underestimation of gas temperatures during the combustion period from single-zone modelling.

One of the most important parts that influence transient response is the fuel injection system. It is strongly suspected that the use of steady state fuel pump curves (as is the case with most transient simulations so far) can be quite limiting in terms of accurate dynamic engine prediction, since the fuel pump experiences a transient operation of its own during the engine speed or load change. To this end, a detailed fuel injection pump submodel, which mathematically analyses the processes inside the fuel pump, will be integrated in the transient simulation code and its results will be compared with those derived using steady state fuel pump curves.

The effect of a detailed, per degree crank angle, modelling of friction components is also focused upon. Friction torque varies significantly during an engine cycle [**12**, **13**]. Its magnitude compared with the brake torque is not negligible, particularly at low loads where the most demanding transient events commence. Friction modelling in transient simulation codes has always been used in the form of mean f.m.e.p. relations, remaining constant for every degree crank angle in each cycle in the model simulation, thus limiting the effect of real friction torque in the predictive capabilities of the model. The sensitivity of the predictions to friction modelling errors was investigated, among other issues, by Watson [**3**]. In the present paper, the more fundamental method proposed by Taraza *et al.* [**13**] is used for analytical modelling of each friction component. This method separates friction torque into four terms, allowing for detailed modelling at each degree crank angle.

Furthermore, during transient operation both friction [**14**] and combustion [**9**, **14**, **15**] are characterized by non-steady state behaviour, differentiating engine response and performance when compared with the corresponding steady state values, at the same engine speed and fuelling conditions. Winterbone and Loo [**1**] assumed that friction torque should be generally overestimated during the transient event by some percentage, to account for the peculiarities of transient operation. This aspect has also been investigated by the present research group for a naturally aspirated compression ignition engine [**6**], where transient friction torque was increased in relation to the instantaneous crankshaft deceleration. Winterbone and Tennant [**14**] found that, during transients initiated from load increases, the mixing process became poorer, probably owing to over-penetration resulting in deposition of fuel on the piston.

A transient diesel engine simulation code has been developed by the present authors that incorporates some important features to account for the peculiarities of the transient operations. Detailed relations concerning fuel injection, combustion, dynamic analysis, heat transfer to the cylinder walls, and turbocharger with aftercooler operation during transient response have been developed and validated [**6**, **7**, **11**].

The sensitivity analysis carried out will be given in a series of diagrams that depict speed as well as other interesting engine variable responses such as fuel pump rack position or boost pressure. Owing to the narrow speed range of the engine in hand, only load increases under a constant governor setting are investigated, which nonetheless play a significant role in the European transient cycles of heavy-duty vehicles [**16**].

2 EXPERIMENTAL STUDY

The experimental investigation was conducted on a heavy-duty, turbocharged, medium-high-speed diesel engine [**17**], the main data of which are given in Table 1.

The first requirement from the engine test bed instrumentation [**18**] was to investigate the steady state performance of the engine in question. For this purpose, an extended series of steady state trials was conducted for preliminary examination of the predictive capabilities of the model and to calibrate successfully the individual submodels. By so doing, estimation of the constants for combustion, heat transfer, friction, and fuel pump simulation was made possible. The matching between experimental and predicted steady state results is given in Fig. 1 and is quite successful for the whole engine operating range, using the same set of submodels constants, thus providing a sound basis for the transient simulation.

The investigation of transient operation was the next task. For the transient tests conducted, the initial speed was 1180 or 1380 r/min and the initial load was 10 per cent of the engine full load. The final conditions for the transient events varied from 47 to 95 per cent of the engine full load [**17**].

A typical example of a conducted transient experiment is given in Fig. 2, for fully warmed-up engine conditions, showing the response of some important first-law properties. Here, the initial load was 10 per cent of the full engine load at 1180 r/min. The final load applied was almost 85 per cent of the full engine load. The application of the final load was effected

Table 1 Basic data for engine and turbocharger

Engine model and type	MWM TbRHS 518S In-line, six-cylinder, four-stroke, compression ignition, turbocharged, aftercooled, heavy-duty
Speed range	1000–1500 r/min
Bore/stroke/swept volume	140 mm/180 mm/16.62 l per cylinder
Compression ratio	17.7 : 1
Maximum power	320 hp (236 kW) at 1500 r/min
Maximum torque	1520 N m at 1250 r/min
Fuel pump	Bosch PE-P series, in-line, six-cylinder with mechanical governor Bosch RSUV 300/900
Turbocharger	KKK M4B 754/345 Single-stage, centrifugal compressor Single-stage, twin-entry, axial turbine
Moment of inertia	Engine and brake: 15.60 kg m^2 Turbocharger: 7.5×10^{-4} kg m^2

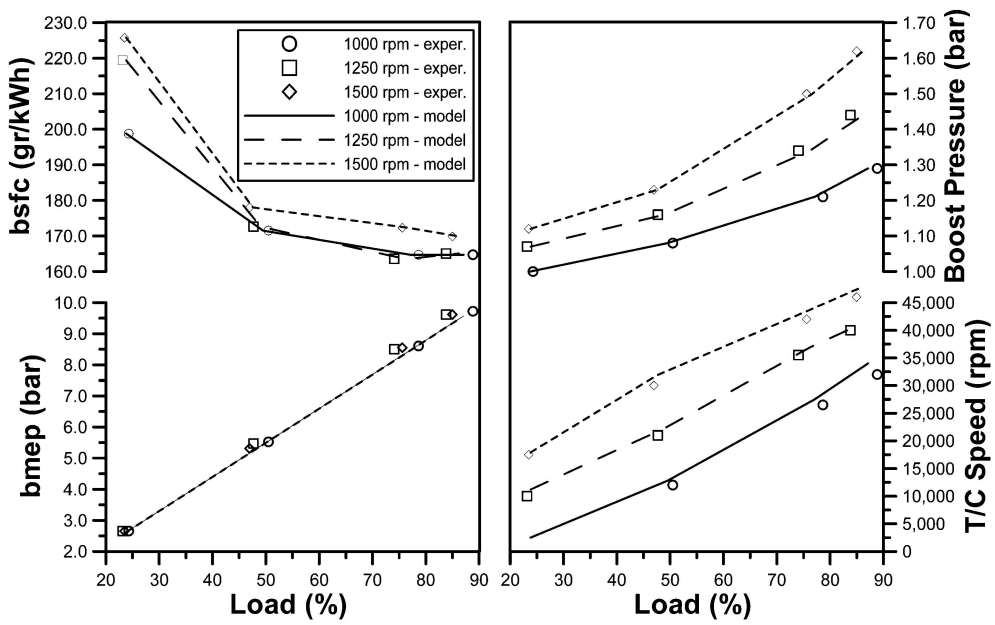

Fig. 1 Experimental and predicted steady state engine operation

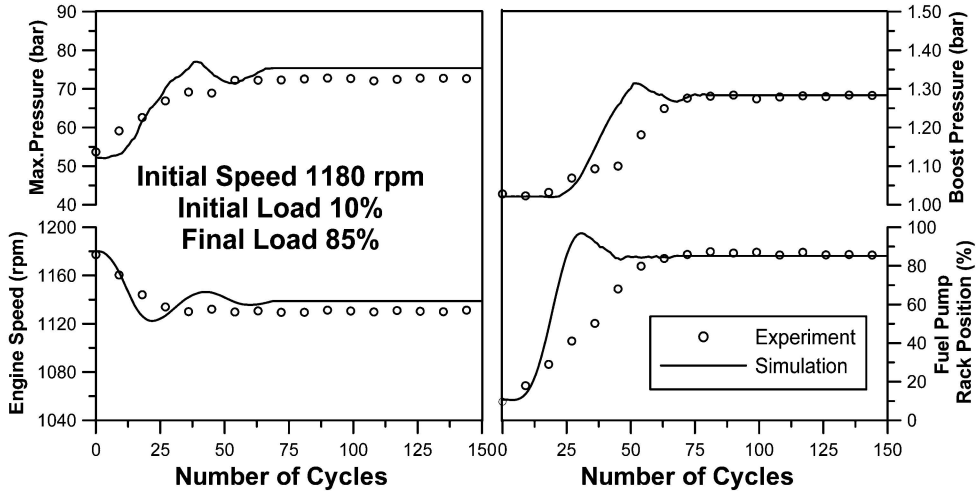

Fig. 2 Experimental and predicted engine transient response to an increase in load

by the movement of the brake control lever, which in turn increased the amount of water inside the brake by appropriately increasing the active surface of the inlet tube. However, this hydraulic brake is characterized by a high mass moment of inertia, of the order of 5.375 kg m^2, resulting in long and non-linear actual load change times and profile. This phenomenon was accounted for in the simulation model by arbitrarily increasing the load application time. The overall matching between experimental and predicted transient responses at final conditions is satisfactory for all engine and turbocharger variables. The fuel pump rack position is notably delayed compared with the speed profile owing to the hysteresis induced by the governor. Boost pressure and, mainly, cylinder maximum pressure are closely correlated with the fuel pump rack position response.

3 SIMULATION ANALYSIS

3.1 General process description

Since the present analysis does not, at the moment, include prediction of exhaust gas emissions and on the other hand deals with transient operation calculations on a degree crank angle basis, a single-zone model is used as a basis for thermodynamic process evaluation. This approach combines satisfactory accuracy with limited PC program execution time. Polynomial expressions from reference [**19**] with a 298 K reference datum are used. They concern evaluation of internal energy and specific heat capacities for first-law application to cylinder contents, using the filling and emptying modelling technique on a degree crank angle basis [**6**, **7**, **19–22**].

3.2 In-cylinder processes

For studying the combustion process, the model proposed by Whitehouse and Way [**20**, **23**] is applied. In this model the combustion process consists of two parts, i.e. a preparation-limited and a reaction-limited (Arrhenius-type) combustion rate. It is vital for a proper simulation of transient response that combustion modelling takes into consideration the continuously changing nature of operating conditions. Thus, constant K, in the (dominant) preparation rate equation of the Whitehouse–Way model, is correlated with the Sauter mean diameter (SMD) of the fuel droplets through a formula of the type $K \propto (1/\mathrm{SMD})^2$ [**20**]. For the evaluation of SMD (μm), an empirical expression proposed by Hiroyasu *et al.* [**24**] is used

$$\mathrm{SMD} = 25.1(\Delta p)^{-0.135} \rho_{\mathrm{g}}^{0.12} V_{\mathrm{tot}}^{0.131} \tag{1a}$$

where Δp is the mean pressure drop across the injection nozzle (MPa) (derived by the fuel pump submodel, which will be described later), ρ_{g} is the density of air at the time injection starts, and V_{tot} is the amount of fuel delivered per cycle and pump stroke (mm^3).

The improved model of Annand [**25**] is used to simulate heat loss Q_{L} to the cylinder walls

$$\frac{\mathrm{d}Q_{\mathrm{L}}}{\mathrm{d}t} = A\left\{\frac{k_{\mathrm{g}}}{D} Re^b \left[a(T_{\mathrm{g}} - T_{\mathrm{w}}) + \frac{a'}{\omega}\frac{\mathrm{d}T_{\mathrm{g}}}{\mathrm{d}t}\right] + c(T_{\mathrm{g}}^4 - T_{\mathrm{w}}^4)\right\} \tag{1b}$$

where a, a', b, and c are constants evaluated after the experimental matching at steady state conditions, k_{g} is the gas thermal conductivity, and the Reynolds number, Re, is calculated with a characteristic length

equal to piston diameter D and a characteristic speed, u_{char}, derived from a k–ε zero-dimensional turbulent kinetic model. It holds [**19**, **26**] that

$$\frac{\mathrm{d}\bar{E}}{\mathrm{d}t} = \frac{1}{2}\frac{\mathrm{d}m}{\mathrm{d}t}u_{\text{inl}}^2 - P - \frac{\bar{E}}{m}\frac{\mathrm{d}m}{\mathrm{d}t} \qquad \text{and}$$

$$\frac{\mathrm{d}k}{\mathrm{d}t} = P - m\varepsilon - \frac{k}{m}\frac{\mathrm{d}m}{\mathrm{d}t} \tag{1c}$$

where $\bar{E} = 0.5m\bar{u}^2$ is the mean flow kinetic energy supplied to the cylinder during the inlet process, which is partially converted to turbulent kinetic energy $k = 1.5mu'^2$ (isotropic turbulence) through a turbulent dissipation process at a rate of $P = 2.7(\rho\sqrt{kD})(\bar{u}^2/D^2)$ and finally to heat through viscous dissipation at a rate of $m\varepsilon$ with $\varepsilon = (k/1.5m)^{1.5}$. The characteristic speed is $u_{\text{char}} = \sqrt{\bar{u}^2 + u'^2}$, which is used in the Reynolds number needed in equation (1b).

The temperature T_{w} used above corresponds to the cylinder liner. Based on previous experimentally validated findings for this type of engine (for example, references [**19**] and [**21**]), the piston crown temperature is assumed to be 50 K higher and the cylinder head temperature 100 K higher than that of the liner as computed from equation (1b).

3.3 Engine dynamics

The conservation of angular momentum applied to the total system (engine plus load) yields [**2**, **4**]

$$\tau_{\text{e}}(\varphi, \omega) - \tau_{\text{load}}(\omega) - \tau_{\text{fr}}(\varphi, \omega)_{\text{trans}} = G_{\text{tot}}\frac{\mathrm{d}\omega}{\mathrm{d}t} \tag{2}$$

where G_{tot} is the engine-brake mass moment of inertia and $\tau_{\text{e}}(\varphi, \omega)$ stands for the instantaneous value of the engine torque. The connecting rod is modelled as a rigid body experiencing reciprocating and rotating movement at the same time [**6**, **7**]. Also, $\tau_{\text{load}}(\omega)$ is the load torque, which, for the hydraulic brake coupled to the engine examined, is $\propto \omega^2$. Lastly, $\tau_{\text{fr}}(\varphi, \omega)_{\text{trans}}$ stands for the friction torque during transient operation, which will be analysed in detail in section 8.

3.4 Turbocharger

The compressor and turbine operating points are evaluated, for every computational step in the engine simulation code, using manufacturer's data at steady state conditions. These maps, which also include turbine isentropic efficiency variation, have been incorporated into the PC code in the form of second-order polynomial expressions [**27**].

4 MULTICYLINDER MODEL

At steady state operation the performance of each cylinder is essentially the same owing to the constant position of the governor clutch resulting in the same amount of fuel being injected per cycle.

At transient operation, on the other hand, each cylinder experiences different fuellings during the same engine cycle owing to the continuous movement of the fuel pump rack, initiated by a load or speed change. These differentiations in fuelling can result in significant differentiations in torque response and finally speed, so affecting significantly the whole engine operation. As regards speed changes, only the first cycles are practically affected, but, when load changes are investigated, significant variations can be experienced throughout the transient cycle.

Contrary to the usual approach, i.e. solution of the governing equations for one cylinder and subsequent use of suitable phasing images of the behaviour of that cylinder, a true multicylinder engine model is developed. Here, all the governing differential and algebraic equations are solved individually for every one cylinder of the six-cylinder engine under study. The dominant variable here is the fuel pump rack position, which moves continuously during the transient event owing to the respective governor clutch movement, thus differentiating the amount of injected fuel per cylinder even in the same cycle.

Apart from this differentiation in fuelling, each cylinder also experiences different air mass flowrates during the same transient engine cycle owing to the transient operation of both turbocharger compressor and inlet manifold. These are taken into account, as both inlet and exhaust manifolds are modelled in the PC code to exchange mass only with that cylinder which experiences inlet or exhaust at the particular computational step. Consequently, no phasing image of the inlet and exhaust process of one cylinder through a 'mean' inlet and exhaust manifold simulation is applied, while at the same time interactions between exhausting cylinders, which can under certain circumstances lead to backflow, are also taken into account. As a consequence, the use of the multicylinder engine model results in different individual cylinder air–fuel ratios during an engine transient cycle owing to the respective differentiation in both air mass flow and fuelling rates.

This 'multicylinder' approach has, of course, the drawback of increasing the computational time almost linearly to the number of cylinders involved, but it is capable of providing more accuracy with the transient operation phenomena. Moreover, it can

offer better results as regards manifold simulation even at steady state conditions. The engine under study, being a six-cylinder one, has a twin-entry turbine. This means that its exhaust manifold consists of two parts, one of which communicates with cylinders 1 to 3 and the other with cylinders 4 to 6. This particular configuration has also been taken into consideration in the simulation results described below.

Figure 3 is a typical representation of the results obtained using the multicylinder engine modelling approach. The total moment of inertia is halved for the sake of this investigation. For the nominal transient case of 10–70 per cent load increase, the response of the relative air–fuel ratio, λ (i.e. the actual air–fuel ratio divided by its stoichiometric value), and the respective maximum (main chamber) pressure of the first and last cylinders in firing order are depicted. The case with 10–95 per cent engine load increase is also given for comparison. Apart from the period where the fuel pump rack position reaches its maximum point, there is a clearly distinguishable difference in the values of λ owing to both fuelling and air quantity differentiations between the cylinders (of the order of 7.5 per cent maximum) during the same engine cycle. Similarly, all other variables that depend on the fuelling rate or air fuel quantity, i.e. instantaneous cylinder pressures, indicated mean effective pressure, blow-by losses, heat flux, bearing loading, etc., are also differentiated from cylinder to cylinder during the same transient cycle, affecting in this way the whole engine transient response.

The above finding is expanded in Fig. 4, where the pressure and temperature diagrams of the same cylinders are depicted for cycles 5 and 15 of the nominal load increase case of 10–70 per cent. Both the pressure and temperature of the main chamber can take up to 5 per cent greater values when the first and the last cylinders in firing order are under investigation.

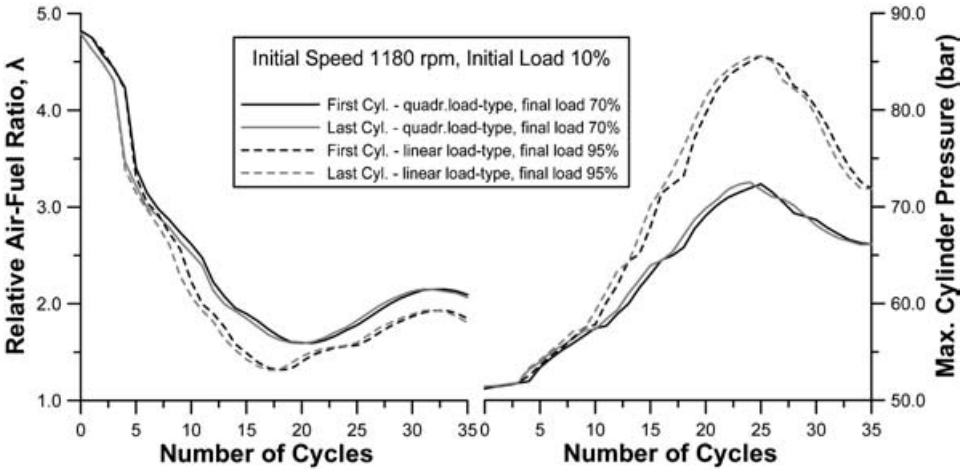

Fig. 3 Response of the first and last cylinders in firing order to an increase in load

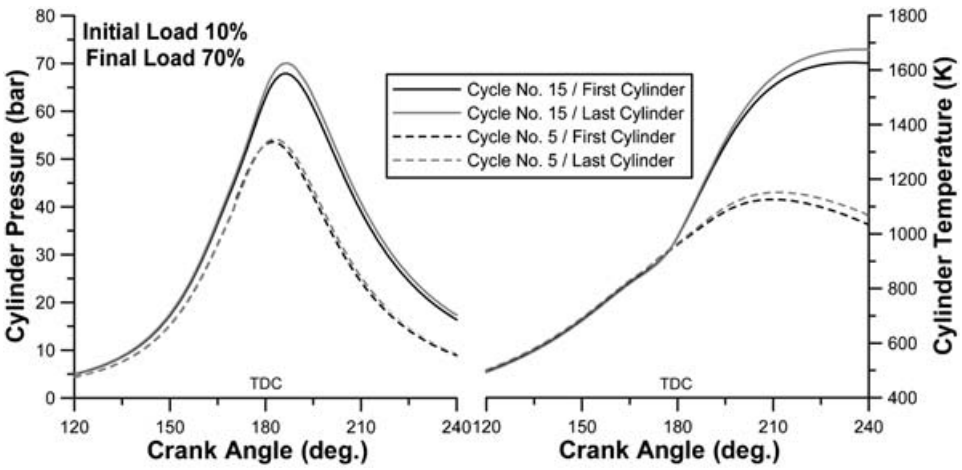

Fig. 4 Main chamber pressure and temperature distribution of first and last cylinders in firing order during specific cycles of transient event

5 CYLINDER WALL TEMPERATURE

The cylinder wall temperature is usually assumed to remain constant during each transient event, since there is not enough time available for it to reach its new steady state conditions. In order to investigate the validity of the constant wall temperature assumption, a detailed heat transfer scheme has been developed to study the temperature distribution from the gas to the cylinder wall up to the coolant (convection from gas to internal wall surface and from external wall surface to coolant, and conduction across the cylinder wall). The one-dimensional unsteady heat conduction equation reads [**19**, **21**] as follows

$$\frac{\partial T}{\partial t} = \frac{1}{\rho_{\mathrm{w}} c_{\mathrm{w}}} \frac{\partial}{\partial x}\left(k_{\mathrm{w}} \frac{\partial T}{\partial x}\right) \tag{3}$$

where ρ_{w} is the wall density and c_{w} is the wall specific heat capacity. Applying the boundary conditions to both wall sides (gas side and coolant side) yields the following equation

$$\frac{\mathrm{d}Q_{\mathrm{L}}}{\mathrm{d}t} = A\frac{k_{\mathrm{w}}}{S_{\mathrm{w}}}(T_{\mathrm{w,g}} - T_{\mathrm{w,c}}) = h_{\mathrm{c}}(T_{\mathrm{w,c}} - T_{\mathrm{c}}) \tag{4}$$

where $\mathrm{d}Q_{\mathrm{L}}/\mathrm{d}t$ is the heat flux computed from equation (1), S_{w} is the cylinder wall thickness, k_{w} is its thermal conductivity, and h_{c} is the heat transfer coefficient from the external wall side (respective temperature $T_{\mathrm{w,c}}$) to the coolant. Equations (4) are solved for the two unknown variables, i.e. the wall temperatures $T_{\mathrm{w,g}}$ and $T_{\mathrm{w,c}}$.

Figure 5 compares the results obtained using the constant wall temperature approach and the analytical heat convection–conduction scheme for the same transient load increase of 10–70 per cent. It is revealed that, although the cylinder wall temperature indeed varies during the transient test, this variation only marginally affects the response of the engine, represented here by its most typical variable, i.e. the crankshaft rotational speed. Thus, the assumption of constant cylinder wall temperature throughout the transient operation can be justified.

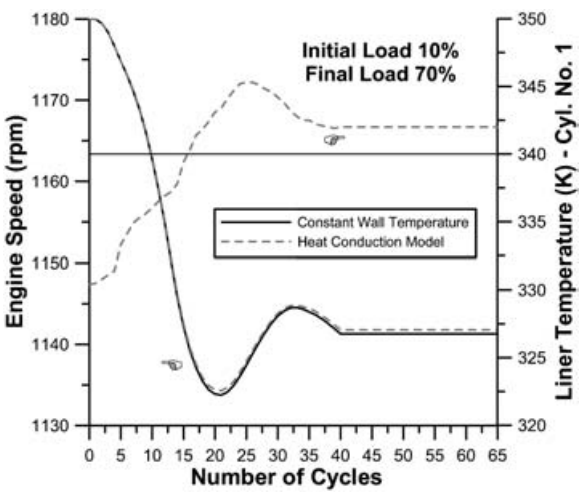

Fig. 5 Comparison of response to an increase in load between detailed and constant cylinder wall modelling

6 RADIATION TEMPERATURE

It is well known that, when single-zone modelling is applied, as is the usual case with transient simulation analyses, good accuracy in the prediction of pressures inside the cylinder can be obtained. This leads to successful estimation of the heat release rate and engine property response during transients. On the other hand, there is a significant underestimation of gas temperatures, which may also limit heat losses and thus engine torque prediction. Some efforts have been made in the past to overcome this drawback of single-zone modelling, which is also responsible for its inability roughly to predict exhaust emission trends. One such approach was proposed by Assanis and Heywood [**26**]. They calculated the apparent radiant temperature, which can be used in the radiation term of equation (1) instead of the gas temperature.

They simulated the radiation temperature as

$$T_{\mathrm{r}} = \frac{T_{\mathrm{g}} + T(\Phi = 1.1)}{2} \tag{5}$$

where the (adiabatic flame) temperature of combustion products at fuel–air equivalence ratio $\Phi = 1.1$ was computed from a correlation of the instantaneous air temperature and pressure of the NASA equilibrium program for constant-pressure hydrocarbon air combustion. The last term on the right-hand side of Annand's heat transfer equation (1) (the radiation term) becomes

$$\left(\frac{\mathrm{d}Q_{\mathrm{L}}}{\mathrm{d}t}\right)_{\mathrm{r}} = A\varepsilon_{\mathrm{a}}\sigma(T_{\mathrm{r}}^4 - T_{\mathrm{w}}^4) \tag{6}$$

where σ is the Stefan–Boltzmann constant and ε_{a} is the apparent grey body emissivity.

Incorporating such an approach in a single-zone model results in an increased range of temperatures in the cylinder during combustion and consequently an increased heat transfer (radiation) contribution. Figure 6 presents the effect of this approach on the predicted transient response of the engine. In the same graph the maximum temperatures of cylinder 1

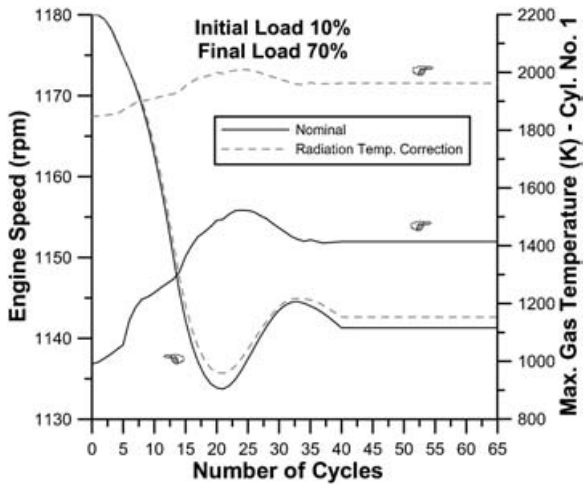

Fig. 6 Comparison of response to an increase in load between conventional and corrected radiation temperature modelling

are depicted, with the nominal temperature found from the conventional analysis that underestimates maximum cylinder temperature by up to 500 K, as can be concluded from the radiation model curve. The effect on the engine speed response is also obvious, affecting both the maximum (5.5 per cent) and the final speed droop (4.2 per cent). However, no distinguishable differences are observed during the first cycles where the fuelling is still kept at low levels.

7 FUEL PUMP OPERATION

The amount of fuel injected per cycle and cylinder, in the majority of the transient simulations, is found by applying the steady state fuel pump curves at the instantaneous values of engine speed and fuel pump rack position of cylinder 1 for every transient cycle. This approach constitutes a rather coarse simplification, since the fuel pump experiences a transient operation of its own during the dynamic conditions of the engine with a very possible differentiation in the amount of injected fuel per cylinder compared with the one under similar (engine speed and fuel pump rack position) steady state conditions. This is in conformity with the experimental remarks made by Murayama *et al.* [**15**].

A mathematical fuel injection model, experimentally validated at steady state conditions, is applied to simulate the fuel pump injector lift mechanism [**28**], taking into account the delivery valve and injector needle motion. The unsteady gas flow equations are solved using the method of characteristics, providing the dynamic injection timing as well as the duration and the rate of injection for each cylinder at each transient cycle. The obvious advantage here is that the transient operation of the fuel pump is also taken into account, through the fuel pump residual pressure, which is built up together with the other variables during the transient event. Moreover, this individual fuel injection subroutine is called upon once for every cylinder at each cycle with the values of angular velocity, fuel pump rack position, and pump residual pressure existing at the point of static injection timing of the individual cylinder. The time burden imposed by the particular subroutine is not of concern, since it is executed in not more than 0.2 s in a typical PC. The results, for application of both fuel injection approaches, are depicted in Fig. 7, where a difference of the order of 8 per cent is observed in the lowest engine speed (and consequently the other engine variables). These confirm the initial suspicions and highlight the importance of incorporating a fuel pump model when dealing with dynamic engine calculations.

8 FRICTION MODELLING

For the calculation of friction inside the cylinder, the method used so far by all other researchers in the

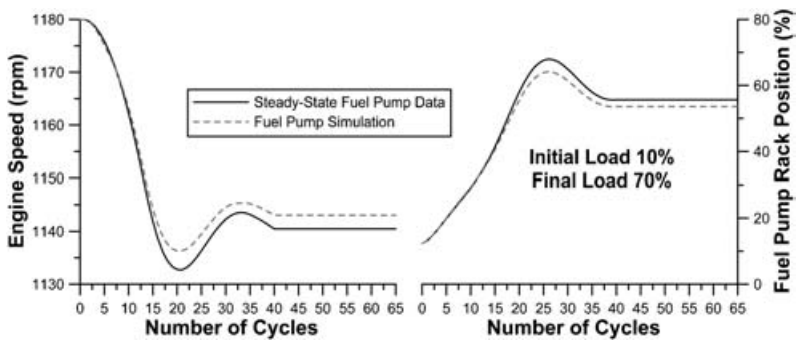

Fig. 7 Comparison of response to an increase in load between steady state and detailed fuel pump modelling

field, i.e. the mean f.m.e.p. approach [**29**], is compared with the detailed method proposed by Taraza *et al.* [**13**]. The latter method describes the non-steady profile of friction torque during each cycle on the basis of fundamental friction analysis. In this method the total amount of friction is divided into four parts, i.e. piston ring assembly, loaded bearings, valvetrain, and auxiliaries. Piston ring friction analysis (including the piston ring and piston skirt contributions) is based on fundamental lubrication theory and was validated with experimental data. It is based on the fact that lubrication is hydrodynamic for most of the piston stroke, with metal contact occurring near 'hot' top dead centre. Bearing friction is mainly hydrodynamic with the deformation of the bearing housing on account of the applied loading playing an important role. Valvetrain friction is governed by friction between cam and tappet and is mainly elastohydrodynamic. Moreover, account of engine oil temperature effects on total friction through the use of oil kinematic viscosity is another important aspect of this friction model. Detailed description of the model can be found in references [**13**] and [**30**]. The total friction torque at each degree crank angle is the sum of the above terms and it varies continuously during the engine cycle, unlike the mean f.m.e.p. equation where friction torque remains constant.

Figure 8 investigates the effect of friction modelling adopted for a 10–95 per cent load change and for a linear load type. Fuel pump rack position and boost pressure response are also depicted for this load change, the load–torque of which is given in the upper right subdiagram. The two speed curves almost coincide only until cycle 15 where the main change in fuelling occurs, a fact leading to differentiations in gas pressure and consequently in the profile of friction torque and thus engine speed. The mean f.m.e.p. results differ by almost 6 per cent as regards final equilibrium speed and consequently in all other engine and turbocharger variable responses. This is due to the considerable underestimation of friction torque around firing TDC that the mean f.m.e.p. assumption induces. Higher load changes and more demanding load types lead to more abrupt governor clutch movements and so greater crankshaft angular decelerations, revealing the differentiation in the predictions from the two friction approaches.

9 DETERIORATION DURING TRANSIENT OPERATION

9.1 Combustion

Murayama *et al.* [**15**] studied the acceleration behaviour of a single-cylinder, naturally aspirated diesel engine. They found that, owing to rapid and considerable changes in fuelling, instantaneous torsional deformations in the driving system of the fuel injection pump were taking place, leading to an incomplete combustion, which steady state combustion modelling was unable to predict.

At the same time, Winterbone and Tennant [**14**], working on a six-cylinder, turbocharged diesel engine, found that the combustion process somehow deteriorated during transient operation after a load increase. They applied the same combustion modelling with the one in this study, i.e. the fundamental Whitehouse–Way approach, and concluded

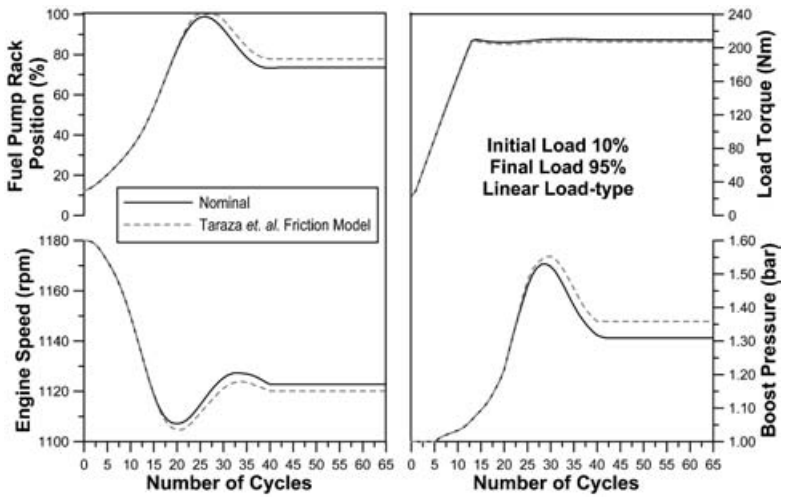

Fig. 8 Comparison of response to an increase in load between mean f.m.e.p. and analytical friction modelling

that the value of preparation rate constant K, which is responsible for the major part of combustion, was reduced during transients, making the whole preparation process slower. This differentiation in transient combustion development has also been confirmed, particularly as regards NO_x emissions, by Cui *et al.* [**9**].

There are usually two approaches applied in the modelling of combustion during transient operation, both acknowledging the importance of an accurate heat release rate pattern. Some researchers prefer to extrapolate the heat release rate from previously recorded experimental pressure diagrams during transient tests, which can afterwards be fed into the simulation code for prediction of transient operations. In the second approach, adopted also by the present research group, a semi-empirical heat release rate law is used, the results of which have already been confirmed under steady state conditions. Great care has to be taken, in this case, with modifications needed in order to take into account the peculiarities of transient combustion, which the steady state modelling cannot predict.

Combining the findings of Winterbone and Tennant [**14**] and Murayama *et al.* [**15**], an investigation is made of the effect of combustion deterioration using a simple equation for correction of the preparation constant during a transient, i.e.

$$K_{\text{trans}} = K_{\text{o}}\left(\frac{\text{SMD}_{\text{o}}}{\text{SMD}}\right)\left[1 - C_{\text{comb}}\frac{m_{\text{finj}} - m'_{\text{finj}}}{m_{\text{finj,max}}}\right] \tag{7}$$

where m_{finj} is the amount of injected fuel quantity over an engine cycle, and m'_{finj} corresponds to the amount of fuel injected in the previous cycle. The value of coefficient C_{comb} needs experimental investigation. Nonetheless, some interesting preliminary results can be found in Fig. 9 where the engine speed response is predicted for three values of C_{comb}, i.e. 0, 4, and 6. The effect of the deterioration of combustion in engine response is shown to have quite a dramatic effect.

9.2 Friction

According to Winterbone and Tennant [**14**], rapid changes in loading lead to instantaneous, though considerable, deflections of the crankshaft owing to great accelerations/decelerations, resulting in an increase in transient mechanical friction. The following correlation is applied for the transient case

$$\tau_{\text{fr}}(\varphi)_{\text{trans}} = \tau_{\text{fr}}(\varphi)\left[1 + C_{\text{fr}}\frac{\varepsilon(\varphi)}{\varepsilon_{\text{max}}}\right] \tag{8}$$

where the instantaneous value for the total friction torque $\tau_{\text{fr}}(\varphi)$ is corrected according to the current crankshaft angular acceleration $\varepsilon(\varphi)$ [**6**, **7**], thus providing the real transient friction torque $\tau_{\text{fr}}(\varphi)_{\text{trans}}$ needed in equation (2). In equation (8), ε_{max} is the hypothetical maximum crankshaft deceleration experienced after applying a 0–100 per cent load change in one cycle. Obviously, its use makes the constant C_{fr} dimensionless. The exact value of coefficient C_{fr} needs experimental investigation, but a hint of its effect is given in Fig. 10 in accordance with the statements of references [**1**] and [**14**]. Clearly, a higher value of C_{fr} leads to greater values of friction torque during the transient event and, thus, to greater speed droops (up to 12 per cent) and positions of the fuel pump rack. In reference [**6**] it was shown that, for a naturally aspirated diesel engine (Ricardo E-6), a value of $C_{\text{fr}} = 1$ compared with $C_{\text{fr}} = 0$ could result in as much as a 25 per cent lower minimum engine speed. In that case, however, the total mass moment of inertia was (proportionally) significantly smaller and the speed range of the engine greater. As a result, the crankshaft deceleration ε assumed greater values.

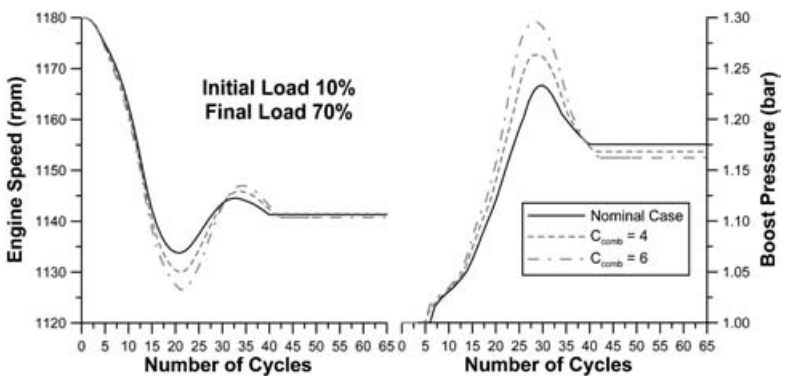

Fig. 9 Comparison of response to an increase in load for three values of the combustion deterioration coefficient

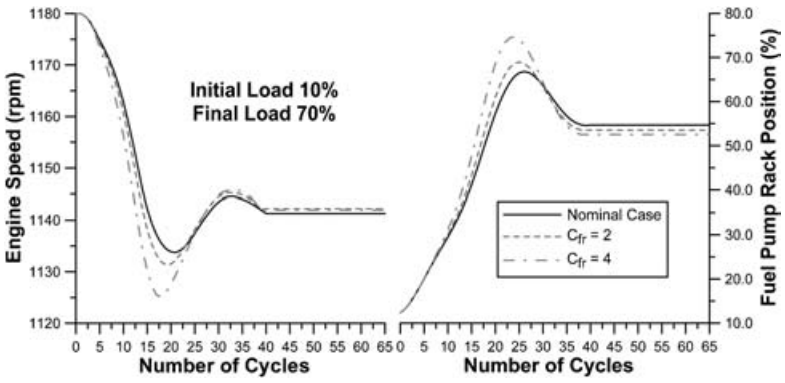

Fig. 10 Comparison of response to an increase in load for three values of the friction deterioration coefficient

10 OTHER USUAL SIMPLIFICATIONS – FUTURE WORK

Work on simplifications (e), (f), and (g) mentioned in section 1 is under development. In particular, as regards turbocharger operation, a 'flattening' of compressor curves during transient operation is accomplished using a differential equation, which takes into account the compressor through-flow time [**31**]. This is believed to represent the transient behaviour of the compressor more accurately.

As regards modelling the brake, it has been shown [**32**] that its transient response differs broadly from the steady state curves, at least as regards variable fill hydraulic dynamometers. This, however, is valid for large speed changes of the order of at least 500 r/min.

Modelling the intake and exhaust manifolds using the method of characteristics [**33**] is also believed to affect the results from the simulations, at least as far as long exhaust pipes are concerned. This will be accompanied with extra PC execution time.

11 CONCLUSIONS

A transient analysis simulation program developed has been used to study the errors induced by various modelling simplifications in the prediction of turbocharged diesel engine transient operation. The usual modelling approaches studied, together with the results from the more sophisticated models and the respective burden in PC execution time, are summarized in Table 2.

Approaches 3 and 4 require extended computer code work, and, moreover, approach 3 increases the PC execution time considerably. Except for

Table 2 Summary of the difference in results and of the PC time burden induced when applying more detailed transient modelling

Simulation section	Usual approach	Examined more detailed approach	Difference in results for current engine set-up	PC time burden
1 In-cylinder calculations	Single-zone modelling	Radiation temperature correction	5.5%	Negligible
2 Cylinder wall temperature	Constant value	Analytical heat convection–conduction scheme	None	Negligible
3 Cylinder–manifolds interdependence	Single-cylinder approach	'Pure' multicylinder approach	7.5%	Considerable
4 Fuel injection	Steady state fuel pump curves	Fuel pump injector mechanism model	8%	Very small
5 Turbocharger	Steady state map	'Flattening' of compressor curves	$\leqslant$1–2%*	Negligible
6 Dynamometer	Steady state curve	Transient modelling of brake	None*	Very small
7 Exhaust manifold	Filling and emptying	Method of characteristics	$<$3%†	Considerable
8 Friction	'Mean' f.m.e.p.	Modelling per °CA	6%‡	Negligible
9 Difference in transient from steady state	No compensation	'Deterioration' in friction/combustion rates	$>$10%	Minimal

*Estimation only – no actual simulations carried out.
†Based on difference in results during steady state operation.
‡For fully warmed-up conditions.

the detailed heat convection–conduction scheme (approach 2), all other approaches prove to have an important effect on the predicted engine response as regards maximum engine speed droop and turbocharger and engine final conditions. As such, they should be included in a transient simulation code.

It is strongly felt that even greater differences between the simplified and the more detailed modelling approaches exist. These could not be revealed owing to the high mass moment of inertia of the engine under study and its narrow speed range.

REFERENCES

1 **Winterbone, D. E.** and **Loo, W. Y.** A dynamic simulation of a two-stroke turbocharged diesel engine. SAE paper 810337, 1981.

2 **Watson, N.** and **Marzouk, M.** A non-linear digital simulation of turbocharged diesel engines under transient conditions. SAE paper 770123, 1977.

3 **Watson, N.** Transient performance simulation and analysis of turbocharged diesel engines. SAE paper 810338, 1981.

4 **Winterbone, D. E.** Transient performance. In *The thermodynamics and gas dynamics of internal combustion engines* (Eds J. H. Horlock and D. E. Winterbone), Vol. 2, 1986 (Clarendon Press, Oxford).

5 **Arcoumanis, C., Megaritis, A.,** and **Bazari, Z.** Analysis of transient exhaust emissions in a turbocharged vehicle diesel engine. In IMechE Conference on *Turbocharging and Turbochargers*, 1994, paper C484/038, pp. 71–81 (Institution of Mechanical Engineers, London).

6 **Rakopoulos, C. D.** and **Giakoumis, E. G.** Simulation and analysis of a naturally aspirated, indirect injection diesel engine under transient conditions comprising the effect of various dynamic and thermodynamic parameters. *Energy Conversion Managmt*, 1998, **39**, 465–484.

7 **Rakopoulos, C. D., Giakoumis, E. G.,** and **Hountalas, D. T.** A simulation analysis of the effect of governor technical characteristics and type on the transient performance of a naturally aspirated IDI diesel engine. SAE paper 970633, 1997; *Trans. SAE, J. Engines*, 1997, **106**, 905–922.

8 **Lindgren, M.** and **Hansson, P. A.** Effects of transient conditions on exhaust emissions from two non-road diesel engines. *Biosyst. Engng*, 2004, **87**, 57–66.

9 **Cui, Y., Deng, K.,** and **Wu, J.** A modeling and experimental study of transient NO_x emissions in turbocharged DI diesel engines. *Proc. IMechE, Part D: J. Automobile Engineering*, 2004 **218**, 535–541.

10 **Rakopoulos, C. D.** and **Giakoumis, E. G.** Availability analysis of a turbocharged diesel engine operating under transient load conditions. *Energy*, 2004, **29**, 1085–1104.

11 **Rakopoulos, C. D., Giakoumis, E. G., Hountalas, D. T.,** and **Rakopoulos, D. C.** The effect of various dynamic, thermodynamic and design parameters on the performance of a turbocharged diesel engine operating under transient load conditions. SAE paper 2004-01-0926, 2004.

12 **Rezeka, S. F.** and **Henein, N. A.** A new approach to evaluate instantaneous friction and its components in internal combustion engines. SAE paper 840179, 1984.

13 **Taraza, D., Henein, N.,** and **Bryzik, W.** Friction losses in multi-cylinder diesel engines. SAE paper 2000-01-0921, 2000.

14 **Winterbone, D. E.** and **Tennant, D. W. H.** The variation of friction and combustion rates during diesel engine transients. SAE paper 810339, 1981.

15 **Murayama, T., Miyamoto, N., Tsuda, T., Suzuki, M.,** and **Hasegawa, S.** Combustion behaviors under accelerating operation of an IDI diesel engine. SAE paper 800966, 1980.

16 http://www.dieselnet.com/standards/cycles/etc.html

17 **Rakopoulos, C. D., Giakoumis, E. G.,** and **Hountalas, D. T.** Experimental and simulation analysis of the transient operation of a turbocharged multi-cylinder IDI diesel engine. *Energy Res.*, 1998, **22**, 317–331.

18 **Zhao, H.** and **Ladommatos, N.** *Engine combustion instrumentation and diagnostics*, 2001 (Society of Automotive Engineers, Warrendale, Pennsylvania).

19 **Heywood, J. B.** *Internal combustion engine fundamentals*, 1988 (McGraw-Hill, New York).

20 **Benson, R. S.** and **Whitehouse, N. D.** *Internal combustion engines*, 1979 (Pergamon Press, Oxford).

21 **Stone, R.** *Introduction to internal combustion engines*, 3rd edition, 1999 (Macmillan, London).

22 **Rakopoulos, C. D., Rakopoulos, D. C., Giakoumis, E. G.,** and **Kyritsis, D. C.** Validation and sensitivity analysis of a two-zone diesel engine model for combustion and emissions prediction. *Energy Conversion Managmt*, 2004, **45**, 1471–1495.

23 **Whitehouse, N. D.** and **Way, R. G. B.** Rate of heat release in diesel engines and its correlation with fuel injection data. *Proc. IMechE, Part 3J*, 1969–70, **184**, 17–27.

24 **Hiroyasu, H., Kadota, T.,** and **Arai, M.** Development and use of a spray combustion modelling to predict diesel engine efficiency and pollutant emissions. *Bull. Jap. Soc. Mech. Engrs*, 1983, **26**, 569–76.

25 **Annand, W. J. D.** and **Ma, T. H.** Instantaneous heat transfer rates to the cylinder head surface of a small compression-ignition engine. *Proc. IMechE*, 1970–71, **185**, 976–987.

26 **Assanis, D. N.** and **Heywood, J. B.** Development and use of a computer simulation of the turbocompounded diesel engine performance and component heat transfer studies. SAE paper 860329, 1986.

27 **Watson, N.** and **Janota, M. S.** *Turbocharging the internal combustion engine*, 1982 (Macmillan, London).

28 **Rakopoulos, C. D.** and **Hountalas, D. T.** A simulation analysis of a DI diesel engine fuel injection system fitted with a constant pressure valve. *Energy Conversion Managmt*, 1996, **37**, 135–150.

29 **Ciulli, E.** A review of internal combustion engine losses. Part 2: studies for global evaluations. *Proc. IMechE, Part D: J. Automobile Engineering*, 1993, **207**, 229–240.

30 **Stanley, R., Taraza, D., Henein, N.,** and **Bryzik, W.** A simplified model of the piston ring assembly. SAE paper 1999-01-0974, 1999.

31 **Fink, D. A., Cumpsty, N. A.,** and **Greitzer, E. M.** Surge dynamics in a free-spool centrifugal compressor system. *Trans. ASME, J. Turbomach.*, 1992, **114**, 321–329.

32 **Hodgson, P. G.** and **Raine, J. K.** Computer simulation of a variable fill hydraulic dynamometer. Part 2: steady state and dynamic open-loop performance. *Proc. IMechE, Part C: J. Mechanical Engineering Science*, 1992, **206**, 49–56.

33 **Rakopoulos, C. D., Andritsakis, E. C.,** and **Hountalas, D. T.** The influence of the exhaust system unsteady gas flow and insulation on the performance of a turbocharged diesel engine. *Heat Recovery Syst. CHP*, 1995, **15**, 51–72.

APPENDIX

Notation

A	surface area (m^2)
BDC	bottom dead centre
°CA	degrees crank angle
D	cylinder bore (m)
E	kinetic energy ($kg\,m^2/s^2$)
f.m.e.p.	friction mean effective pressure (bar)
G	mass moment of inertia ($kg\,m^2$)
h	heat transfer coefficient ($W/m^2\,K$)
k	thermal conductivity (W/m K) and turbulent kinetic energy ($kg\,m^2/s^2$)
K	combustion model preparation rate constant
m	mass (kg)
N	engine speed (r/min)
p	pressure (Pa)
P	turbulent dissipation rate ($kg\,m^2/s^3$)
Q	heat loss (J)
r	crank radius (m)
SMD	Sauter mean diameter (μm)
t	time (s)
TDC	top dead centre
T	absolute temperature (K)
u	velocity (m/s)
V	volume (m^3)
ε	crankshaft angular acceleration (s^{-2}) and viscous dissipation rate (m^2/s^3)
λ	relative air–fuel ratio
ρ	density (kg/m^3)
τ	torque (N m)
φ	crank angle measured from the BDC position (deg)
Φ	fuel–air equivalence ratio
ω	angular velocity (rad/s)

Subscripts

c	coolant
e	engine
fr	friction
g	gas
r	radiation
trans	transient
w	wall